Thermal Performance Evaluation of Solar PV Cooling Model with Rectangular Winglet Pair Vortex Generator Application

Rizky Cahyo Setiawan
Department of Mechanical Engineering, Faculty of Engineering, Universitas Sebelas Maret

Indri Yaningsih
Department of Mechanical Engineering, Faculty of Engineering, Universitas Sebelas Maret

Dominicus Danardono Dwi Prija Tjahjana
Department of Mechanical Engineering, Faculty of Engineering, Universitas Sebelas Maret

Aditya Rio Prabowo
Department of Mechanical Engineering, Faculty of Engineering, Universitas Sebelas Maret

他

https://doi.org/10.5109/7342439

出版情報：Evergreen. 12 (1), pp.71-80, 2025-03. 九州大学グリーンテクノロジー研究教育センター
バージョン：

Thermal Performance Evaluation of Solar PV Cooling Model with Rectangular Winglet Pair Vortex Generator Application

Rizky Cahyo Setiawan[1], Indri Yaningsih[1,*], Dominicus Danardono Dwi Prija Tjahjana[1,*], Aditya Rio Prabowo[1], Koji Enoki[2], Kyaw Thu[3], Takahiko Miyazaki[3]

[1]Department of Mechanical Engineering, Faculty of Engineering, Universitas Sebelas Maret, Jl. Ir. Sutami 36 A, Surakarta 57126, Indonesia

[2]Graduate School of Mechanical and Intelligent Systems Engineering, The University of Electro-Communications, 1-5-1 Chofungaoka, Chofu, Tokyo 152-8585, Japan

[3]Department of Energy and Environmental Engineering, Interdisciplinary Graduate School of Engineering Sciences, Kyushu University, 6-1 Kasuga-koen, Kasuga-shi, 816-8580, Fukuoka, Japan

*Author to whom correspondence should be addressed:
E-mail: indriyaningsih@staff.uns.ac.id (IY); ddanardono@staff.uns.ac.id (DDDPT)

(Received August 28, 2024; Revised January 9, 2025; Accepted January 9, 2025).

Abstract: The temperature of solar photovoltaic (PV) panels increases due to solar irradiation, which leads to decreased power generation. To decrease the temperature, an improvement in convective cooling is needed. It can be achieved by airflow modification using a vortex generator (VG). This study investigated the effect of a rectangular-shaped winglet vortex generator (RWVG) on the performance of a solar PV model. The RWVG was designed with four different attack angles, configured in a common flow-up orientation. The attack angles (β) were adjusted from 30º, 50º, 60º, and 70º. Additionally, the Reynolds numbers (Re) were varied under 724, 1086, 1448, and 1810. The experimental setup was equipped with a thermal camera to capture the temperature distribution on the solar PV model surface. Results indicated that the solar PV equipped with the RWVG at an attack angle of β = 50° exhibited the highest performance, showing a 30.85% improvement in the convection heat transfer coefficient and a thermal performance enhancement of 1.36 times. As the Reynolds number increased, performance tended to improve within the variations studied. Visual observations confirmed that the RWVG at β = 50° achieved the greatest temperature reduction, approximately 21.1%.

Keywords: solar PV; RWVG; configuration; angle of attack; Reynolds number

1. Introduction

Solar photovoltaic (PV) is one of the best choices for revolutionizing the renewable energy field[1]. The crossing of the equator line in Indonesia[2] is very suitable for developing solar PV. However, the increasing temperature of solar PV due to solar irradiation becomes the main challenge when applying solar PV since it causes a decrease in energy conversion efficiency[3]. Several studies have tried to use active and passive cooling methods. Bayrak et al.[4] performed active cooling on solar PV using Phase Change Material (PCM), thermoelectricity, and aluminum fins. Meanwhile, Jakhar et al.[5] conducted Centering Photovoltaic (CPV) with the help of active cooling. Basically, active cooling methods require a lot of additional mechanical equipment, which would improve the external power input. This further increases the cost and maintenance requirements[6]. Therefore, passive cooling is advantageous because it eliminates additional equipment and power input.

Passive cooling is a cost-effective or accessible technology strategy focusing on available resources without energy consumption[7,8]. Vortex generators (VGs) are considered a good technique for convection heat transfer improvement for solar PV[9]. It could produce vortices that can accelerate fluid momentum exchange, thereby improving fluid thermal uniformity[10]. Passive techniques with VGs can create elongated vortices in fluid flow, inducing disruptive secondary flows and reducing boundary layer thickness[11,12]. Many forms of VGs have been used to develop vortices that absorb thermal energy[13]. However, winglet-type VGs produce excellent and promising vortices that can persist further downstream of the surface[14].

VGs can be found abundantly in heat exchanger (HE) systems. Xie et al.[15] revealed that improving finned tube HE performance can be achieved primarily using the VGs. Some types of HE equipped with VG were found in solar thermal system[16]. The role of VG, in this case, can improve the temperature performance of the convection airflow[17]. In addition, using VG has become a topic of interest in aerodynamic applications. In unsteady aerodynamic problems, VGs suppress the dynamic stall of wind turbine airfoils[18].

Different shapes of VG winglet type were placed inside a circular tube on a solar collector, in the form of delta and rectangular. Their effect on the solar collector performance was analyzed by da Silva et al.[19]. The modeling results show that they effectively increase thermal efficiency. In addition, they were appropriate for low Reynolds numbers. Between those two shapes of VGs, the delta winglet pair was found to have an excellent Nusselt number than the rectangular one, according to Tang et al.[20]. The study was done under the condition that the Reynolds number was more than 3.000.

Solar air heater performance with rectangular winglet vortex generator (RWVG) pairs was investigated by Dezan et al.[21]. The VG arrangement was the main interest of their study. They found that the robust vorticity structure was more developed on flow-up RWVG pairs configuration than the flow-down. The changes in the flow structure due to the vorticity would enhance the heat transfer mechanism. Accordingly, Wang et al.[22] also verified that by using rectangular winglets with a flow-up configuration, the heat transfer was enhanced by about 10 - 23% higher than in other configurations. This occurred in the cooling channel of a plate-type fuel element.

Samadifar et al.[23] evaluate the heat transfer improvement on HE systems using rectangular VG with simple shapes, which was enhanced by 7%[23]. However, pressure drops further affect the system[23,24] as compensation for heat transfer enhancement. The improvement of the heat transfer mechanism using VG was described by Kashyap et al.[25]. An elongated vortex was formed due to surface modification using RWVG. The convection heat transfer rate was improved since the vortex directly affected the boundary layer within the systems. Naik et al.[26] investigated an air duct's heat transfer and flow properties containing a curved RWVG. The heat transfer inside the air duct was increased by 39.4% when concave RWVG with a 90º angle of attack was installed in the air duct. Syaiful et al.[27] also found that the concave RWVG improved the thermal performance with a maximum value of 129.75% compared to the baseline.

The thermal performance of the fin-tube HE equipped with two shapes of longitudinal VG, in the form of rectangular and delta winglets, was tested numerically by Li et al.[28]. They found that as compared to those without VGs, the presence of VGs enhances the thermal performance. In addition, rectangular winglets perform better than delta winglets. He et al.[29] studied numerically the effect of modified RWVG pairs on the performance of fin-tube HE. The modification includes VG configuration and number of rows, Reynolds number, and angle of attack. The interesting finding was the RWVG pairs enhanced the heat transfer performance with small pressure drop values. Additionally, the performance improved with the increase in rows and attack angle.

The effective positioning of the attack angle of vortex generators (VG) plays a critical role in enhancing heat transfer. In a study conducted by Oh and Kim[30], the impact of the attack angle on the heat transfer performance of fin-tube heat exchangers was thoroughly analyzed for three distinct curved winglet VG configurations: rectangular, delta-upstream, and delta-downstream. It was observed that changes in the attack angle significantly influence the flow, particularly in the development of wake region and secondary flow, thereby enhancing heat transfer. According to their findings, maintaining the attack angle below 90° is paramount for ensuring optimal heat transfer performance. The research also highlighted the potential for up to a 75% improvement in comparison to conventional VGs.

The lapping fins model has been identified as a highly effective passive technique for solar PV cooling modules. In conditions of 1000 W/m^2 average solar radiation and a 33 ºC ambient temperature, passive cooling through this method has exhibited superior performance, resulting in a lower average temperature than the reference PV about 24.6 ºC[31].

As a passive cooling method, a VG is being explored as a potentially cost-efficient for PV module cooling. The research delves into the impact of using curved VGs to enhance flow characteristics in the wake area behind a tube. Studies by Gong et al.[32] and Lin et al.[33] have shown that curved VGs (rectangular winglet[32] and delta winglet[33]) effectively reduce the wake area behind the tube and create a secondary flow to improve heat transfer. Additionally, the height, length, and placement of the curved VG also play a role in influencing heat transfer performance.

Wang et al.[34] and Lei et al.[35] suggest that an optimal aspect ratio (length/height) of the delta winglet VG is 2. Similarly, according to Mohanakrishnan et al.[36], heat transfer enhancement occurs when the transverse distance between VGs is 2 times the winglet height, which induces a strong downwash. The study also explains that the winglet height is taken as the characteristic length because it directly affects the resulting vortical flow structure, leading to increased heat transfer.

Several of the aforementioned studies indicate that vortex generators (VGs) have undergone extensive development and are commonly utilized to augment heat transfer within a system. However, the utilization of VGs for solar photovoltaic (PV) cooling remains infrequent, particularly concerning the influence of wind direction, which can significantly impact the temperature distribution during solar PV cooling. This current study explores the thermal performance assessment of a solar PV cooling model employing a Rectangular Winglet Vortex Generator (RWVG) by adjusting the attack angle (β) to emulate the wind approach towards the solar PV panels. The variation of β was arranged by 30º, 50º, 60º, and 70º. Moreover, the RWVG was set up in a paired configuration with a shared upward flow direction towards the air inlet. The research utilized a low Reynolds number, adjusted to under 2,000. The study will analyze the convective heat transfer coefficients and thermal performance. Additionally, temperature distribution visualization will be obtained using a thermal camera to bolster the data results.

2. Methods

2.1 Test Apparatus Setup

A test apparatus for conducting the thermal performance evaluation for the solar PV cooling model is illustrated in Fig. 1.

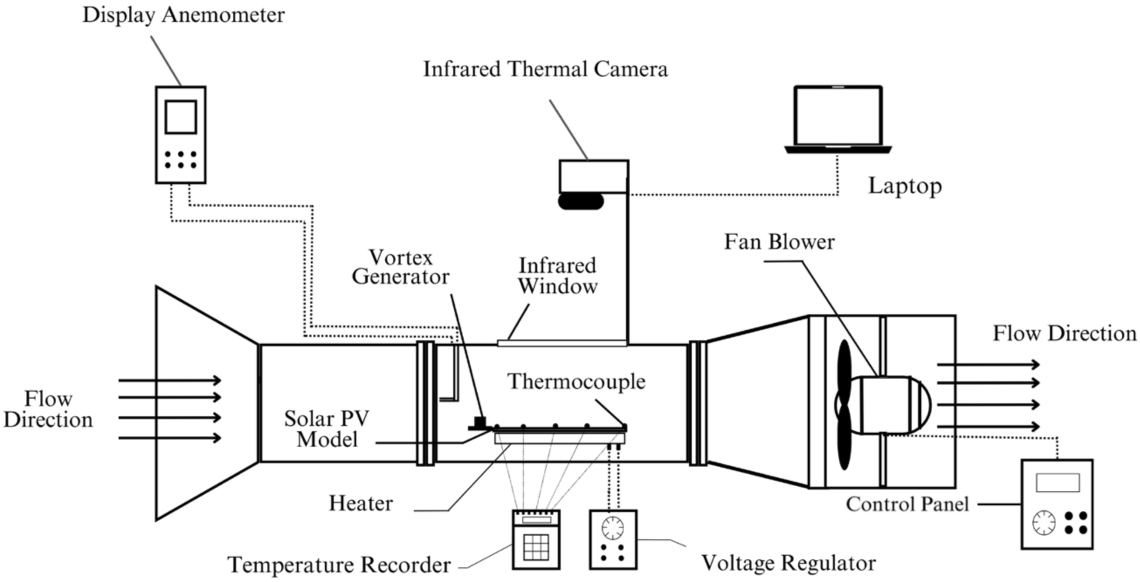

Fig. 1: Experimental setup

The subsonic wind tunnel system consists of an inlet, contraction cone, test section, diffuser, blower, and outlet. The test section contains a solar PV model and RWVG. The upper side of the test section is equipped with an infrared window that is transparent to the surface of the solar PV model. The clear window provides functions for the thermal camera to capture the surface temperature distribution of the solar PV model in the test. This system also has a blower that circulates air to the test section. The blower is an axial fan with an induction motor with a power of 4 kW , which can provide airflow with a maximum speed of up to 30 m/s. The control panel was used to adjust the blower speed so that the air could flow steadily across the test section.

The RWVG used in the current study was made of a stainless-steel plate with a thickness (b) 0.1 mm. The geometry of RWVG is illustrated in Fig. 2. In Figure 2(a), the placement of the RWVG pair configuration is shown, with a common flow direction directed upwards towards the air. The RWVG was positioned just in front of the solar PV model, and a circle highlights a detailed view of the RWVG's geometry. The distance of the rear RWVG (denoted as B) was measured at 14.775 mm for each pair of winglets, with the distance between the winglet pairs (denoted as w) set at 29.95 mm. The RWVG had a thickness of 0.5 mm. Figure 2(b) depicts the airflow approaching the RWVG, and additional details of the RWVG pair's geometry are also provided. The RWVG has a length (L) of 29.95 mm and a height (H) of 14.775 mm. The aspect ratio was optimized to a value of 2. There are two pairs of RWVG winglets in this test. A partition made of insulation was used between the RWVG pair and the inlet of the solar PV model to prevent any direct contact between the RWVG and the solar PV model.

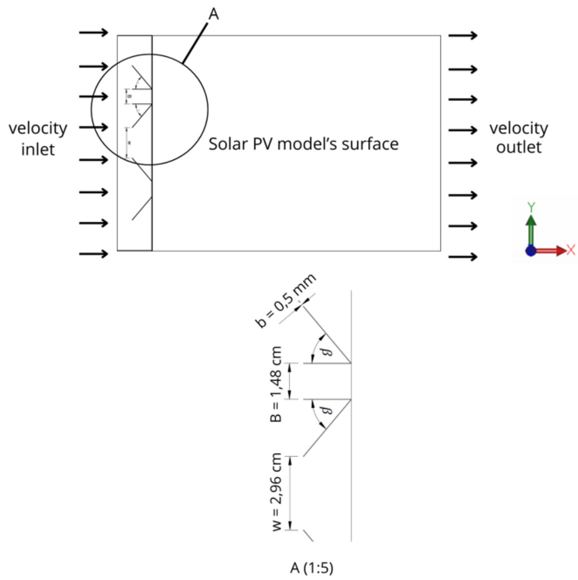

(a)

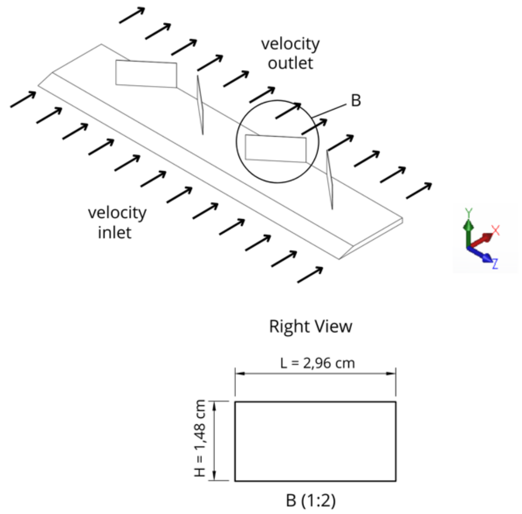

(b)

Fig. 2: Details of rectangular winglet vortex generator (RWVG) Geometry; (a) RWVG placement on solar PV model, (b) Airflow direction on the RWVG.

The illustration in Figure 3 depicts the solar PV model, designed with a surface consisting of a 3mm-thick flat plate aluminum alloy A1100 measuring 310 x 210 mm. This sizing was chosen to accommodate the constraints of the Subsonic Wind Tunnel test section. A 1200 W capacity heater was strategically placed under the PV model surface to emulate solar radiation intensity. The bottom cover of PV model, constructed from plywood and lined with 40 mm thick glass wool aluminum foil, acts as a heat insulator capable of isolating heat up to 121 ºC. This measure was implemented to safeguard the solar PV model from the cooling effects of airflow. To regulate the heat generated by the heater, an OKI Voltage Regulator type TDGC2-2000 with a maximum output voltage of 250 VAC is employed, ensuring a constant heat flux received by the solar PV model.

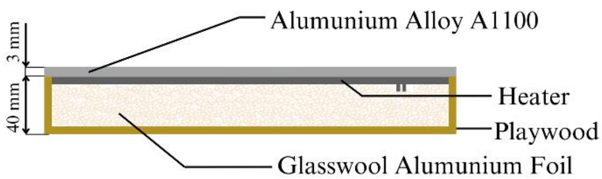

Fig. 3: Solar PV model

Five T-type thermocouples were attached on the surface of the solar PV model from the inlet to the end of the outlet with a distance of 80 mm between thermocouples. T-type thermocouples have a temperature range from 0º to 200 ºC. The thermocouple was connected to the data acquisition system (temperature recorder) to read the measurement results. The temperature recorder used in this test was Lutron BTM-4208SD, with a data reading accuracy of ±0.4%. The velocity inlet was set as 0.8, 1.2, 1.6, and 2 m/s. A Benetech GT8907 Digital Anemometer was used to measure the velocity inlet. It can measure velocities between 0.4 to 25 m/s with an accuracy of ±3.5%.

2.2 Relationship between Convection Heat Transfer Equation and Testing

The analysis in this study utilizes constant heat flux as one of the boundary conditions for heat transfer. The following equation defines the heat flux:

$$q'' = \frac{V_{electric} \cdot I}{A_S} \quad (1)$$

q'' represent the heat flux (W/m^2), $V_{electric}$ represent the heater voltage (V), I represent the heater current (A), and A_S represent the surface area of the solar PV model (m^2). The heater's heating of the solar PV model is adjusted to the heat flux received in Surakarta City, Central Java, Indonesia. The amount of heat flux calculated is then applied to the surface area of the solar PV model.

The evaluation of heat transfer performance involves the calculation of the convection heat transfer coefficient. This is achieved through analysis of the heat flux data in conjunction with the surface temperature of the solar PV model. The convection heat transfer coefficient is calculated by:

$$h = \frac{q''}{(T_S - T_\infty)} \quad (2)$$

h denotes the convection heat transfer coefficient ($\mathrm{W/m^2 \cdot K}$), q'' represents the heat flux (W/m^2), T_s corresponds to solar PV model surface temperature (K), and T_∞ stands for the room temperature (K).

The Reynolds number (Re) in this test can be calculated through the air velocity variations using the following equation:

$$Re = \frac{VH}{v} \quad (3)$$

V represent air velocity (m/s), H represent RWVG height (m), and v represent kinematic viscosity (m^2/s). According to Mohanakrishnan et al.[36] , RWVG height is used as the characteristic length because it directly affects the development of vortical flow structure.

The Nusselt number (Nu) is directly related to the convection heat transfer coefficient, which can be derived using the following equation:

$$Nu = \frac{hH}{k} \quad (4)$$

h symbolizes the convection heat transfer coefficient ($W/m^2 \cdot K$), H represents the RWVG height (m), and k denotes the thermal conductivity ($W/m \cdot K$).

The concept of thermal performance within convection heat transfer denotes the system's capability to conduct or retain heat. This dimensionless parameter holds significant importance, as it facilitates the application of data collected from surfaces exposed to convective conditions in determining thermal performance. Within the scope of this study, thermal performance specifically encompasses the ratio of the Nusselt number with and without RWVG, and its calculation is as follows:

$$\eta = \frac{Nu_{VG}}{Nu_0} \qquad (5)$$

η represent the thermal performance, Nu_{VG} represent the Nusselt number resulting from the addition of RWVG and Nu_0 corresponds to the Nusselt number without the addition of RWVG.

2.3 Infrared Thermography

Temperature changes on the top surface of the solar PV model were visualized using a FLIR C5 thermal camera. This specific device generates a thermal image wherein varying colors represent different temperatures. Positioned 0.4 m above the surface of the solar PV model, the camera has a resolution of 160 x 120 pixels. Additionally, the FLIR Thermal Studio software was employed to process the infrared images from the thermal camera. The resulting image furnishes the data required to support a comparison of thermal performance enhancement through the addition of the RWVG pair configuration, functioning with a common flow-up direction, to the solar PV model.

3. Result and Discussion

3.1 Effect of Vortex Generator Configuration on Convection Heat Transfer Coefficient

The discussion focuses on the convection heat transfer coefficient across the solar PV model's surface and the behavior of the working fluid when the RWVG pair configuration with a common flow-up direction is introduced. The data calculations are based on a constant power output of 70 W, which is derived from heat flux calculations conducted in Surakarta City. As presented in Figure 4, the RWVG pair configuration with a common flow-up direction increases the convection heat transfer coefficient. It is observed that as the angle of attack increases, the convection heat transfer coefficient also rises. the configuration at a 70º angle of attack with a Reynolds number (Re) of 1810 achieves the highest convection heat transfer coefficient value of 43.49 W/(m²K). Conversely, the lowest coefficient occurs at a 60º angle of attack with a Re of 724, measuring at 25.79 W/(m²K). Increasing the angle of attack of the RWVG strengthens the vortical structures in the wake of the winglets[37]. Additionally, the contact time between the RWVG and the fluid at lower temperatures increases, thereby enhancing heat transfer between them. The most significant increase in the heat transfer coefficient 51.1% is observed at an angle of attack of 50º with a Re of 724. In contrast, the lowest increase, at only 7.35%, occurs at an angle of attack of 30º with a Re of 1810. Overall, these findings align with the research conducted by Daniel et al.[21], indicating that the RWVG configuration with a common flow-up direction generates a robust vorticity structure that enhances heat transfer.

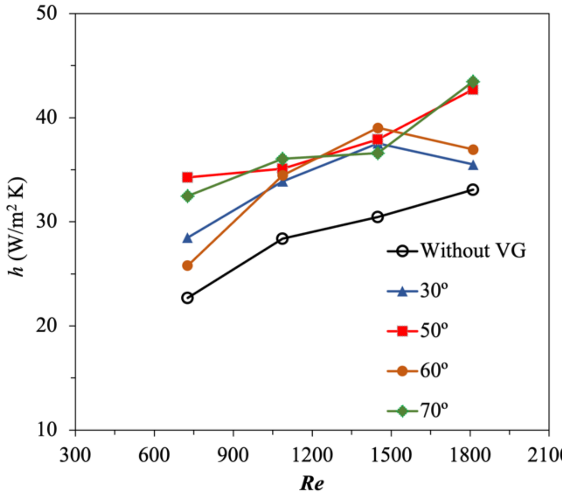

Fig. 4: Effect of angle of attack for RWVG pair with a common flow-up configuration on convective heat transfer coefficient.

From Fig. 4, it is also indicated that as the Reynolds number increases, the convective heat transfer across all variations improves. With a rise in the Reynolds number, the strength of the vortices increases, while the secondary flows along the channel weaken due to the viscosity diffusion of the fluid[38]. This process ultimately enhances the heat transfer rate. However, at attack angles of 30º and 60º, heat transfer starts to decrease when the Reynolds number exceeds 1448. It is interesting to know that uncommon behavior is revealed within this study. The longitudinal vortex development certainly depends on the incoming flow towards the geometry of the VG. RWVG has a sharp surface area, which guides the airflow and determines two parallel uniform streams behind the RWVG. Over time, a region of strong vorticity forms at the frontal surface of the RWVG. However, the fluid velocity behind the RWVG becomes quite slow, creating a wake. This energy dissipation limits the size and intensity of the vortical regions[39]. At attack angles of 30º and 60º, the formation of vortices is not significantly affected, leading to a reduction in the number of vortices and a decrease in the convection heat transfer value.

3.2 Effect of Vortex Generator Angle of Attack Variation on Thermal Performance

The effect of the angle of attack variation of RWVG pair configuration with a common flow-up direction to the solar PV model is illustrated in Fig.5. RWVG pair with an angle of attack of 50º and Re = 724 shows the highest thermal performance with a value of 1.58. It can also be seen from Fig. 5 that with an angle of attack of 30º at Re = 1810, RWVG shows the lowest thermal performance with a value of 1.08.

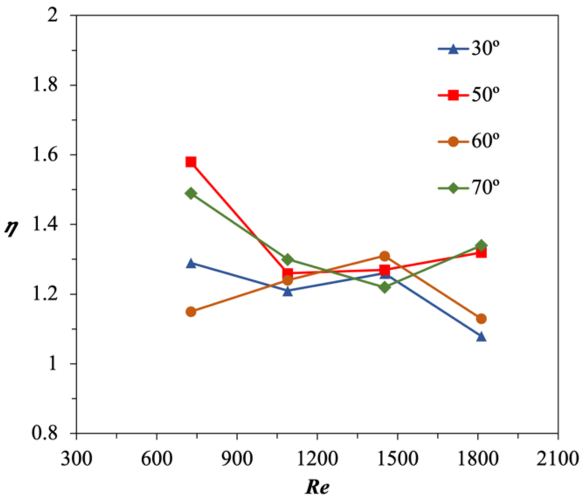

Fig. 5: Effect of angle of attack for RWVG pair with a common flow-up configuration on thermal performance.

In this study, the optimal combinations of the angle of attack and Re for implementing RWVGs were found to be 60° at $Re = 1448$ and 70° at $Re = 1086$. However, the most effective angles for enhancing the thermal performance of the solar PV model were observed at Re = 1810, specifically at 50° and 70° angles of attack. The 50° angle of attack facilitates greater fluid mixing and a thinner boundary layer, resulting in superior performance compared to all other configurations tested.

Additionally, RWVG pair with a common flow-up configuration with a 30º angle of attack does not significantly improve the thermal performance at every Reynolds number tested. In contrast, the 30º and 60º angles of attack showed increased thermal performance at $Re = 1086$ and $Re = 1448$, respectively. Two pairs of RWVGs with a common flow-up configuration provide a fairly good thermal performance improvement effect at $Re = 1088$ throughout the angle of attack variation test. Among attack angle variations, the 50º angle of attack in the pair with a common flow-up configuration shows the best thermal performance numbers when tested with all variations of Reynolds numbers. The results depend on the type of vortices generated. According to Fiebig[40], when the angle of attack is small, the generated vortices are primarily longitudinal; conversely, when the angle of attack is large, they produce more transverse vortices. Longitudinal vortices are generally more effective than transverse vortices[40].

3.3 Thermal Result

The thermal camera was used to investigate the temperature distribution on the solar PV cooling model as the effect of RWVG addition. Hence, the temperature distribution with and without RWVG can be compared. Fig. 6 shows the surface temperature distribution of the solar PV model without RWVG attachment. The RWVG creates secondary flow, altering the temperature field and thinning the thermal boundary layer, which increases the heat transfer rate[38]. The Figures prove that as the Reynolds number increases, the surface temperature of the solar PV model decreases. Without the installation of RWVG, the most dominant temperature drop is located at the inlet of the PV model surface. At the same time, the outlet does not get an optimal cooling effect. It is due to the heat generated by the heater being transferred to the surface of the solar PV model and then carried by convection from the cooling fluid flowing over the surface.

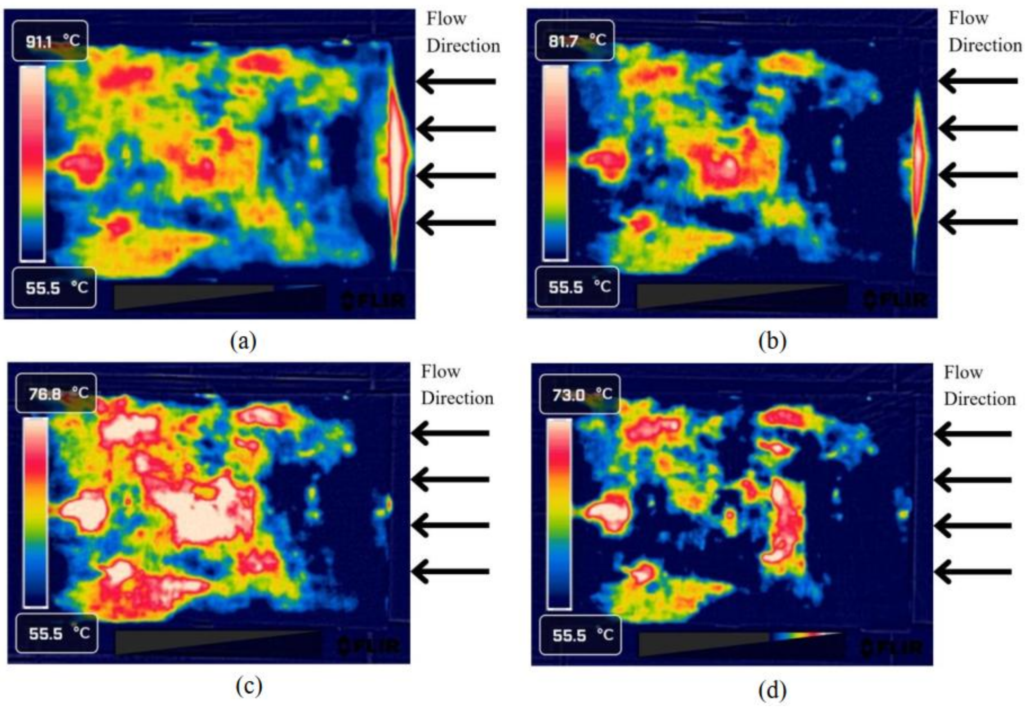

Fig. 6: Surface temperature distribution of solar PV without RWVG under conditions (a) $Re = 724$, (b) $Re = 1086$, (c) $Re = 1448$, (d) $Re = 1810$.

The surface temperature distribution of the solar PV model without VG at Re = 724 is shown in Fig. 6(a). When viewed at the center and outlet of the solar PV model surface, there is no significant decrease in temperature. The temperature recorder detected the highest temperature, reaching 91.1 ºC under the Reynolds number of 724. Fig. 6(b) shows a significant temperature drop at the inlet solar PV model surface. As the Reynolds number increases to 1086, the center and outlet surfaces decrease in temperature compared to the previous condition. At Re = 1086, the temperature recorder detected the highest temperature, reaching 81.7 ºC. The more the Reynolds number increases, the more the surface temperature decreases in all parts. This can be seen in Fig. 6(c) for Re = 1448, with the highest temperature detected by the temperature recorder reaching 76.8 ºC. Figure 6(d) shows the temperature distribution at Re = 1810, where it can be seen that most areas of the solar PV model show a decrease in temperature. The temperature recorder detected the highest temperature at this Reynolds number condition was 73 ºC. The outlet surface of the solar PV model before the addition of the RWVG pair with a common flow-up configuration shows a decrease in temperature that was considered insignificant in all Reynolds number conditions tested.

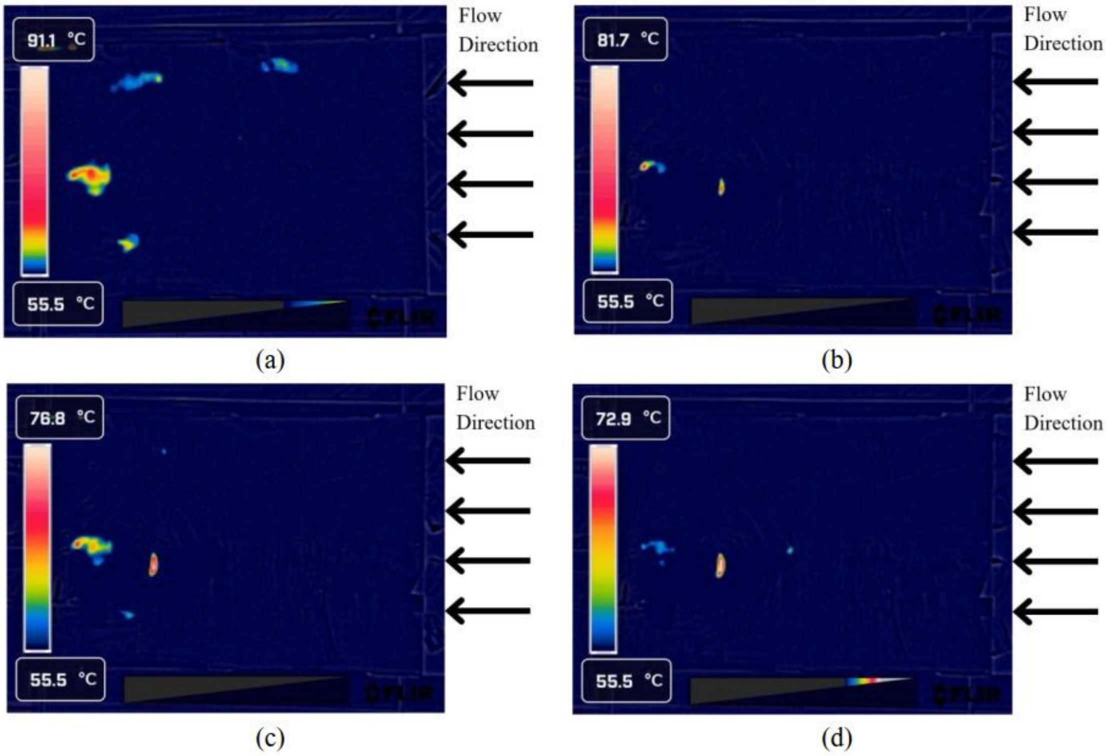

Fig. 7: Highest temperature distribution of RWVG pair with a common flow-up configuration (a) β = 50º (Re = 724), (b) β = 70º (Re = 1086), (c) β = 60º (Re = 1448), (d) β = 70º (Re = 1810).

The addition of an RWVG pair with a common flow-up configuration has the effect of increasing the temperature drop on all parts of the surface of the solar PV model, as shown in Fig. 7. In this figure, four images show the best temperature drop in each Reynolds number condition. Figure 7(a) shows the surface temperature distribution with an angle of attack of 50º. This angle of attack provides a strong vorticity effect at Re = 724, resulting in a 21.6% decrease in the average surface temperature. Figure 7(b) shows the surface temperature distribution with an angle of attack of 70º under Re of 1086. The decrease in average surface temperature under these conditions is 12.5%. Figure 7(c) shows the surface temperature distribution with an angle of attack of 60º under Re of 1448. In this condition, there is a decrease in average surface temperature of 12.6%. Figure 7(d) shows the surface temperature distribution with an angle of attack of 70º under Re of 1810, with an average surface temperature decrease of 13.2%. These four figures have proven that RWVG with pair common flow up configuration could improve convection heat transfer compared to without RWVG. The figures also show that the entire surface of the solar PV model decreases in temperature due to the airflow disturbed by the RWVG when passing through the inlet.

4. Conclusions

An experimental investigation was undertaken to examine the influence of the angle of attack of an RWVG pair with a common flow-up configuration on solar PV cooling. Testing on a solar PV model using various Reynolds numbers (724, 1086, 1448, and 1810) revealed increased convection heat transfer. The results demonstrated that the installation of RWVG led to a rise in the convection heat transfer coefficient on the surface of the solar PV model. Notably, the highest increase in convection heat transfer coefficient, reaching 51.1%, was observed with an attack angle (β) of 50º at Re = 724. Additionally, the installation of RWVG with two pairs resulted in the highest thermal performance, achieving a value of 1.58 at Re = 724, accompanied by a noteworthy decrease in the average surface temperature of the solar PV model by 21.6%, as recorded by the temperature recorder.

Furthermore, it was found that the lowest increase in convection heat transfer coefficient occurred with β = 30º at Re = 1810, reaching only 7.35%. Under the same conditions, the lowest thermal performance was recorded at 1.08. The findings suggest that RWVG with an attack angle of 50º delivers the most effective convection heat transfer for all tests conducted in the RWVG pair with a common flow-up configuration.

Acknowledgments

The research was generously funded through a PNBP grant from Universitas Sebelas Maret, Indonesia, with contract number 194.2/UN27.22/PT.01.03/2024 under the International Collaboration (KI-UNS) scheme.

Nomenclature

q''	heat flux (W/m^2)
$V_{electric}$	voltage of the heater (V)
I	electric current of the heater (A)
A_S	surface area of the solar PV model (m^2)
h	convection heat transfer coefficient ($W/m^2 \cdot K$)
T_s	surface temperature of the solar PV model (K)
T_∞	room temperature (K)
Re	Reynolds number (–)
V	air velocity (m/s)
H	RWVG height (m)
v	kinematic viscosity (m^2/s)
Nu	Nusselt number (–)
k	thermal conductivity ($W/m \cdot K$)
Nu_{VG}	Nusselt number resulting from the addition of RWVG (–)
Nu_0	Nusselt number without the addition of RWVG (–)

Greek symbols

β	angle of attack (º)
η	Thermal performance (–)

References

1) I. Vinoth Kanna, and D. Pinky, “Solar research – a review and recommendations for the most important supplier of energy for the earth with solar systems,” *International Journal of Ambient Energy*, 41 (*8*) 962–968 (2020). doi:10.1080/01430750.2018.1472658.
2) Presiden Republik Indonesia, “Peraturan presiden nomor 22 tahun 2017 tentang ruen,” *Peraturan Presiden*, 1–103 (2017). https://www.esdm.go.id/assets/media/content/content-rencana-umum-energi-nasional-ruen.pdf. (accessed May 24, 2024).
3) R. Rabie, M. Emam, S. Ookawara, and M. Ahmed, “Thermal management of concentrator photovoltaic systems using new configurations of phase change material heat sinks,” *Solar Energy*, 183 632–652 (2019). doi:10.1016/J.SOLENER.2019.03.061.
4) F. Bayrak, H.F. Oztop, and F. Selimefendigil, “Experimental study for the application of different cooling techniques in photovoltaic (pv) panels,” *Energy Convers Manag*, 212 (*March*) 112789 (2020). doi:10.1016/j.enconman.2020.112789.
5) S. Jakhar, M.S. Soni, and N. Gakkhar, “Historical and recent development of concentrating photovoltaic cooling technologies,” Renewable and Sustainable Energy Reviews, 60 41–59 (2016). doi:10.1016/j.rser.2016.01.083.
6) A. Maleki, A. Haghighi, M. El Haj Assad, I. Mahariq, and M. Alhuyi Nazari, “A review on the approaches employed for cooling pv cells,” *Solar Energy*, 209 170–185 (2020). doi:10.1016/J.SOLENER.2020.08.083.
7) X. Zhang, A. Ding, H. Sun, and E. Rahman, “Thermodynamic limits and performance optimization of nighttime thermoradiative energy conversion systems with non-idealities,” *Case Studies in Thermal Engineering*, 45 102932 (2023). doi:10.1016/J.CSITE.2023.102932.
8) V.M. Maytorena, J.F. Hinojosa, S. Moreno, and D.A. Buentello-Montoya, “Thermal performance analysis of a passive hybrid earth-to-air heat exchanger for cooling rooms at mexican desert climate,” *Case Studies in Thermal Engineering*, 41 102590 (2023). doi:10.1016/J.CSITE.2022.102590.
9) I. Arianmehr, D.S.K. Ting, and S. Ray, “Assisted turbulence convective heat transfer for cooling the photovoltaic cells,” *ASME 2013 Heat Transfer Summer Conf. Collocated with the ASME 2013 7th Int. Conf. on Energy Sustainability and the ASME 2013 11th Int. Conf. on Fuel Cell Science, Engineering and Technology, HT 2013*, 1 (2013). doi:10.1115/HT2013-17210.
10) X. Li, P. Yan, J. Wang, and T. Yang, “Effect of novel vortex generator on parabolic trough solar collectors using ionic liquid,” *Appl Therm Eng*, 236 (*PD*) 121830 (2024). doi:10.1016/j.applthermaleng.2023.121830.

11) M. Fiebig, "Vortices, generators and heat transfer," *Chemical Engineering Research and Design*, 76 (*2*) 108–123 (1998). doi:10.1205/026387698524686.
12) A.L. Heyes, and D.A.R. Smith, "Modification of a wing tip vortex by vortex generators," *Aerosp Sci Technol*, 9 (*6*) 469–475 (2005). doi:10.1016/J.AST.2005.04.003.
13) A.A. Alshammari, E.M. Salilih, E. Almatrafi, and M. Rady, "Polymeric coatings for passive radiative cooling of pv modules in hot and humid weather: design, optimization, and performance evaluation," *Case Studies in Thermal Engineering*, 57 (*January*) 104341 (2024). doi:10.1016/j.csite.2024.104341.
14) H. Wu, D.S.K. Ting, and S. Ray, "The effect of delta winglet attack angle on the heat transfer performance of a flat surface," *Int J Heat Mass Transf*, 120 117–126 (2018). doi:10.1016/J.IJHEATMASSTRANSFER.2017.12.030.
15) C. Xie, G. Yan, Q. Ma, Y. Elmasry, P.K. Singh, A.M. Algelany, and M. Wae-Hayee, "Flow and heat transfer optimization of a fin-tube heat exchanger with vortex generators using response surface methodology and artificial neural network," *Case Studies in Thermal Engineering*, 39 102445 (2022). doi:10.1016/J.CSITE.2022.102445.
16) H. Karkaba, S. Russeil, J. V. Simo Tala, D. Bougeard, J. Boonaert, L. Etienne, U. Pelay, and S. Lecoeuche, "Effect of using multiple vortex generator rows on heat transfer enhancement inside an asymmetrically heated rectangular channel," *Appl Therm Eng*, 227 120359 (2023). doi:10.1016/J.APPLTHERMALENG.2023.120359.
17) S.A. Gandjalikhan Nassab, Y. Sheikhnejad, and M. Foruzan Nia, "Novel design of natural solar air heat for higher thermal performance utilizing porous vortex generator," *Thermal Science and Engineering Progress*, 33 101385 (2022). doi:10.1016/J.TSEP.2022.101385.
18) C. Zhu, Y. Feng, X. Shen, Z. Dang, J. Chen, Y. Qiu, Y. Feng, and T. Wang, "Effects of the height and chordwise installation of the vane-type vortex generators on the unsteady aerodynamics of a wind turbine airfoil undergoing dynamic stall," *Energy*, 266 (*November 2022*) 126418 (2023). doi:10.1016/j.energy.2022.126418.
19) F.A.S. da Silva, D.J. Dezan, A. V. Pantaleão, and L.O. Salviano, "Longitudinal vortex generator applied to heat transfer enhancement of a flat plate solar water heater," *Appl Therm Eng*, 158 (*April*) 113790 (2019). doi:10.1016/j.applthermaleng.2019.113790.
20) L.H. Tang, W.X. Chu, N. Ahmed, and M. Zeng, "A new configuration of winglet longitudinal vortex generator to enhance heat transfer in a rectangular channel," *Appl Therm Eng*, 104 74–84 (2016). doi:10.1016/J.APPLTHERMALENG.2016.05.056.
21) D.J. Dezan, A.D. Rocha, L.O. Salviano, and W.G. Ferreira, "Thermo-hydraulic optimization of a solar air heater duct with non-periodic rows of rectangular winglet pairs," *Solar Energy*, 207 (*July*) 1172–1190 (2020). doi:10.1016/j.solener.2020.06.112.
22) Q. Wang, Q. Chen, L. Wang, M. Zeng, Y. Huang, and Z. Xiao, "Experimental study of heat transfer enhancement in narrow rectangular channel with longitudinal vortex generators," *Nuclear Engineering and Design*, 237 (*7*) 686–693 (2007). doi:10.1016/J.NUCENGDES.2006.09.003.
23) M. Samadifar, and D. Toghraie, "Numerical simulation of heat transfer enhancement in a plate-fin heat exchanger using a new type of vortex generators," *Appl Therm Eng*, 133 (*November 2017*) 671–681 (2018). doi:10.1016/j.applthermaleng.2018.01.062.
24) O. Heriyani, M. Djaeni, Syaiful, and A.K. Putri, "Perforated concave rectangular winglet pair vortex generators enhance the heat transfer of air flowing through heated tubes inside a channel," *Results in Engineering*, 16 (*October*) 100705 (2022). doi:10.1016/j.rineng.2022.100705.
25) U. Kashyap, K. Das, and B.K. Debnath, "Effect of surface modification of a rectangular vortex generator on heat transfer rate from a surface to fluid: an extended study," *International Journal of Thermal Sciences*, 134 (*May*) 269–281 (2018). doi:10.1016/j.ijthermalsci.2018.08.020.
26) H. Naik, S. Tiwari, and H.D. Kim, "Flow and thermal characteristics produced by a curved rectangular winglet vortex generator in a channel," *International Communications in Heat and Mass Transfer*, 135 (*May*) 106103 (2022). doi:10.1016/j.icheatmasstransfer.2022.106103.
27) Syaiful, G. Rachmandala, B. Yunianto, M.S.K. Tony Su, and M. I. Maulana, "Heat transfer enhancement with considering pressure loss penalty of airflow through heated plate mounted by perforated concave rectangular winglet vortex generators," *IOP Conf Ser Mater Sci Eng*, 506 (*1*) (2019). doi:10.1088/1757-899X/506/1/012062.
28) L. Li, X. Du, Y. Zhang, L. Yang, and Y. Yang, "Numerical simulation on flow and heat transfer of fin-and-tube heat exchanger with longitudinal vortex generators," *International Journal of Thermal Sciences*, 92 85–96 (2015). doi:10.1016/J.IJTHERMALSCI.2015.01.030.
29) Y.L. He, P. Chu, W.Q. Tao, Y.W. Zhang, and T. Xie, "Analysis of heat transfer and pressure drop for fin-and-tube heat exchangers with rectangular winglet-type vortex generators," Appl Therm Eng, 61 (2) 770–783 (2013). doi:10.1016/J.APPLTHERMALENG.2012.02.040.
30) Y. Oh, and K. Kim, "Effects of position and geometry of curved vortex generators on fin-tube heat-exchanger performance characteristics," *Appl Therm Eng*, 189 116736 (2021). doi:10.1016/j.applthermaleng.2021.116736.

31) A.M. Elbreki, A.F. Muftah, K. Sopian, H. Jarimi, A. Fazlizan, and A. Ibrahim, “Experimental and economic analysis of passive cooling pv module using fins and planar reflector,” *Case Studies in Thermal Engineering*, 23 (*August 2020*) 100801 (2021). doi:10.1016/j.csite.2020.100801.
32) B. Gong, L.B. Wang, and Z.M. Lin, “Heat transfer characteristics of a circular tube bank fin heat exchanger with fins punched curve rectangular vortex generators in the wake regions of the tubes,” *Appl Therm Eng*, 75 224–238 (2015). doi:10.1016/J.APPLTHERMALENG.2014.09.043.
33) Z.M. Lin, C.P. Liu, M. Lin, and L.B. Wang, “Numerical study of flow and heat transfer enhancement of circular tube bank fin heat exchanger with curved delta-winglet vortex generators,” *Appl Therm Eng*, 88 198–210 (2015). doi:10.1016/J.APPLTHERMALENG.2014.11.079.
34) Y. Wang, T. Zhao, Z. Cao, C. Zhai, Y. Zhou, W. Lv, T. Xu, and S. Wu, “Numerical study on the forced convection enhancement of flat-roof integrated photovoltaic by passive components,” *Energy Build*, 289 113063 (2023). doi:10.1016/J.ENBUILD.2023.113063.
35) Y.G. Lei, Y.L. He, L.T. Tian, P. Chu, and W.Q. Tao, “Hydrodynamics and heat transfer characteristics of a novel heat exchanger with delta-winglet vortex generators,” *Chem Eng Sci*, 65 (*5*) 1551–1562 (2010). doi:10.1016/J.CES.2009.10.017.
36) S.K. Mohanakrishnan, Y. Yang, D.S.K. Ting, and S. Ray, “The effect of transverse spacing of a winglet pair on flat plate heat convection,” *Appl Therm Eng*, 194 (*March*) 117094 (2021). doi:10.1016/j.applthermaleng.2021.117094.
37) A. Lemouedda, M. Breuer, E. Franz, T. Botsch, and A. Delgado, "Optimization of the angle of attack of delta-winglet vortex generators in a plate-fin-and-tube heat exchanger," *Int. J. Heat Mass Transf.*, 52 *(November)* 5386-5399 (2012). doi:10.1016/j.ijheatmasstransfer.2010.07.017.
38) A. Abdollahi, and M. Shams, "Optimization of shape and angle of attack of winglet vortex generator in a rectangular channel for heat transfer enhancement," *Appl Therm Eng.,* 81 *(April)* 376-387 (2015). doi:10.1016/j.applthermaleng.2015.01.044.
39) O. Sano, “Vortex Formation behind an Object,” *Forma 30* S75-S76 (2015). doi:10.5047/forma.2015.s012.
40) M. Fiebig, "Embedded vortices in internal flow: heat transfer and pressure loss enhancement," *Int. J. Heat. Fluid Flow*. 16 376-388 (1995). doi:10.1016/0142-727X(95)00043-P.